Iranian Journal of Basic Medical Sciences
ijbms.mums.ac.ir

Imperatorin alleviates post-infarction cardiac fibrosis via the CD44/PI3K/AKT pathway in mice

Hui Yuan [1, 2], YanKun Hao [1], Mohammed Alaa Abdulzahra [3, 4], YueYing Yuan [1], Xuan Li [1], Javeria Qadir [5], ManYu Wang [1], YuanYuan Zhang [1], TingTing Li [1], Jian Sun [6, 1*]

[1] School of Basic Medical Sciences, Mudanjiang Medical University, Mudanjiang 157011, P.R. China
[2] School of Stomatology, Mudanjiang Medical University, Mudanjiang 157011, P.R. China
[3] DNA Research Center, University of Babylon, Hilla 51001, Iraq
[4] Department of Pharmacy, AlAmal College for Specialized Medical Sciences, Karbala -56001, Iraq
[5] Department of Biological Sciences, International Islamic University Islamabad, Islamabad 04436, Pakistan
[6] Collaborative Innovation Center of Development and Application of North Medicine Resources in Mudanjiang City, Mudanjiang 157011, P.R. China

ARTICLE INFO

Article type:
Original

Article history:
Received: May 20,
Accepted:

Keywords:
CD44
Imperatorin
Myocardial fibrosis
Myocardial infarction
PI3K/AKT

ABSTRACT

Objective(s): This study examines the effects of imperatorin (IMP) on cardiac fibrosis in mice with myocardial infarction (MI) and seeks to elucidate the underlying molecular mechanisms.

Materials and Methods: C57BL/6 mice were randomly assigned to a control group, an ISO-induced MI group, and ISO+IMP treatment groups (7.5, 15, and 30 mg/kg). 4D-FastDIA-based quantitative proteomics was used for global proteomic analysis to identify differentially expressed proteins (DEPs) and signaling pathways involved in the anti-fibrotic effects of IMP following MI. Echocardiography was performed to evaluate cardiac function; histopathological analysis and serological indicators were used to assess myocardial injury; and Western blotting was employed to verify the expression and mechanisms of related proteins.

Results: Compared with the ISO group, IMP treatment markedly improved electrocardiographic abnormalities, reduced serum LDH and cTn-I levels, enhanced cardiac function, and attenuated myocardial injury and fibrosis. Proteomic analysis identified 98 DEPs in the ISO/Control group and 127 DEPs in the ISO+IMP/ISO group. GO and KEGG analyses showed that these DEPs were mainly enriched in fibroblast proliferation-related biological processes and ECM-receptor interaction pathways, with significant involvement of the PI3K/AKT signaling pathway. PPI network analysis highlighted FN1, VTN, Col2α2(I), Col1α1(III), and CD44 as key regulatory proteins, among which CD44 was notably down-regulated by IMP. Molecular docking demonstrated strong binding affinity between IMP and CD44. Western blot results further confirmed that IMP significantly reduced the expression of fibrosis-related proteins and suppressed activation of the CD44/PI3K/AKT signaling pathway.

Conclusion: IMP ameliorates myocardial fibrosis in MI mice by modulating the CD44/PI3K/AKT signaling pathway.

▶ Please cite this article as:
Yuan H, Hao Y, Abdulzahra MA, Yuan Y, Li X, Qadir J, Wang M, Zhang Y, Li T, Sun J. Imperatorin alleviates post-infarction cardiac fibrosis via the CD44/PI3K/AKT pathway in mice. Iran J Basic Med Sci 2026; 29:

Introduction

Cardiac fibrosis is a common pathological feature in the progression of various cardiovascular diseases (CVDs)(1). Activated fibroblasts contribute to this process by secreting abundant fibrogenic factors and extracellular matrix (ECM) components, such as fibronectin (FN) and collagen (2). The continuous accumulation of these substances in the interstitial and perivascular spaces leads to increased ventricular wall stiffness and progressive cardiac dysfunction, culminating in heart failure. Due to the limited regenerative capacity of adult cardiomyocytes, the infarcted myocardial tissue after MI is replaced by fibrotic tissue, thereby causing cardiac dysfunction and heart failure. Evidence indicates that anti-remodeling and anti-fibrotic interventions reduce the risk of sudden cardiac death in patients with heart failure (3). Therefore, therapeutic interventions aimed at suppressing cardiac fibrotic remodeling may provide an effective strategy for preventing heart failure in patients with MI.

Imperatorin, a naturally occurring coumarin compound, is abundant in various medicinal plants, including Angelica dahurica and Angelica pubescens, and exhibits multiple biological activities, including anti-inflammatory, antioxidant, and cardioprotective effects (4, 5). Research has demonstrated that IMP can alleviate cardiac hypertrophy in mice by activating the endothelial nitric oxide synthase (eNOS) signaling pathway, thereby preventing heart failure (6). Additionally, IMP exerts myocardial-protective effects in MI by inhibiting the ACE-AngII-AT1R axis (7). These findings suggest that IMP may exert cardiovascular protective effects by ameliorating myocardial fibrosis and suppressing adverse cardiac remodeling. However, its specific impact on MI and myocardial fibrosis, as well as

*Corresponding author: Jian Sun. School of Basic Medical Sciences, Mudanjiang Medical University No. 3 Tongxiang Street, Ai Min District, Mudanjiang 157011, Heilongjiang Province, P.R. China. Email: mdjsunjian@126.com

the underlying mechanism of action, still remains elusive. The isoproterenol (ISO)-induced MI model is a widely used experimental approach for investigating myocardial injury and cardiac remodeling. This model reproduces several key pathological characteristics of human MI. Mechanistically, excessive ISO stimulation increases myocardial workload and oxygen consumption, resulting in an imbalance between oxygen supply and demand and subsequent myocardial hypoxia. Moreover, catecholamine-induced oxidative stress and the autoxidation of catecholamine metabolites may contribute to hemodynamic instability, including hypotension, thereby exacerbating myocardial injury (8, 9).

In the present study, we established an ISO-induced mouse model of MI and employed an integrated strategy combining 4D-FastDIA quantitative proteomics, molecular docking, and experimental validation to elucidate the cardioprotective mechanisms of imperatorin. Unlike previous studies that primarily focused on predefined signaling pathways using hypothesis-driven approaches, our study utilized an unbiased quantitative proteomic strategy to identify potential molecular regulators underlying IMP-mediated cardiac protection. This approach revealed the CD44/PI3K/AKT signaling axis as a critical mediator of cardiac fibrosis and myocardial remodeling. Therefore, we aimed to comprehensively investigate the protective effects of IMP against post-infarction cardiac fibrosis and clarify the molecular mechanisms associated with the CD44/PI3K/AKT pathway. Our findings provide new insights into the therapeutic potential of IMP and offer experimental evidence supporting its application in MI prevention and treatment.

Materials and Methods

Experimental animals and grouping

Specific-pathogen-free (SPF) male C57BL/6 mice, aged 8-10 weeks and weighing 22-25 g, were provided by the Comparative Medicine Center of Mudanjiang Medical University. The mice were housed in a temperature- and humidity-controlled environment (23±1 °C) with a 12 hr light/dark cycle and had free access to sterilized standard chow and drinking water. All animal experimental protocols were approved by the Institutional Animal Care and Use Committee of Mudanjiang Medical University (Approval No. IACUC-20230619-93) and were conducted in accordance with the Guide for the Care and Use of Laboratory Animals published by the National Institutes of Health (NIH).

After one week of acclimatization, mice were randomly assigned to five experimental groups (n=7 per group) using a random number generation method to minimize allocation bias. Control group: Mice were administered 0.5% sodium carboxymethyl cellulose (CMC-Na; 0.1 ml/10 g body weight) by gavage for 15 days and received subcutaneous injections of saline from day 7 to day 15 of the experiment. ISO model group: Mice were administered 0.5% CMC-Na by gavage for 15 days and were subcutaneously injected with isoproterenol (ISO; 50 mg/kg body weight; Sigma-Aldrich, USA) twice at a 24-h interval from day 7 to induce the MI model (10, 11). ISO+IMP 7.5/15/30 mg/kg groups: Mice were administered the corresponding IMP doses intragastrically for 15 days and were subcutaneously injected with isoproterenol, following the same protocol as the ISO model group, to establish the MI treatment model. Animals were excluded from subsequent analyses if they died before sample collection or developed severe health conditions unrelated to the experimental procedures. Samples were collected on days 1 and 7 after model establishment for subsequent experiments (Figure 1A).

Echocardiographic analysis

On days 1 and 7 after model establishment, all mice were anesthetized with 1% isoflurane. A Vivid 7-dimensional echocardiograph (MyLab Delta-vet Esaote, Italy) was used to measure left ventricular ejection fraction and fractional shortening (LVEF and LVFS), left ventricular end-diastolic and end-systolic diameters (LVIDd and LVIDs), and left ventricular wall thickness (LVAWd, LVAWs, LVPWd, and LVPWs) through the transverse axis view. All echocardiographic examinations were performed by an experienced investigator who was blinded to the experimental group allocation. Measurements were obtained from three consecutive cardiac cycles and averaged for subsequent statistical analysis.

Detection of serological indicators

Serum samples were collected on days 1 and 7 after model establishment. The expression levels of lactate dehydrogenase (LDH), cardiac troponin-I (cTnI), malondialdehyde (MDA), and superoxide dismutase (SOD) were detected respectively, in accordance with the kit

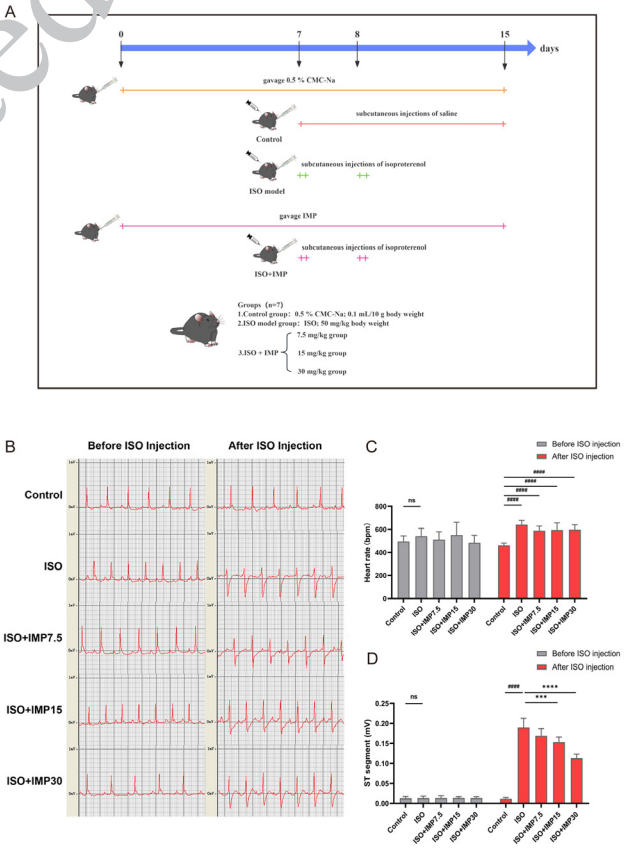

Figure 1. Effects of imperatorin (IMP) on the waveforms of electrocardiograms in mice before and after isoproterenol (ISO) injection
(A) Schematic illustration of the animal experimental protocol; (B) Representative electrocardiogram (ECG) traces of each group before and after ISO injection; (C) Statistical analysis of heart rate (bpm) in each group before and after ISO injection; (D) Statistical analysis of ST segment displacement (mV) in each group before and after ISO injection. ($^{####}P<0.0001$ vs Control, $^{***}P<0.001$, $^{****}P<0.0001$ vs ISO, n=7)

instructions provided by Nanjing Jiancheng Bioengineering Institute (Nanjing, China). All measurements were performed in accordance with standardized protocols, and the investigators responsible for biochemical analyses were blinded to the experimental group allocation. Each sample was analyzed in duplicate, and the average value was used for subsequent statistical analysis.

Histopathological analysis

After the mice were anesthetized, their hearts were quickly excised, fixed in 4 % paraformaldehyde, embedded in paraffin, and sectioned into 4 μm slices. Histological staining was performed for morphological observation, including hematoxylin-eosin (HE) staining and Masson's trichrome staining (Solarbio, Beijing, China). The stained sections were observed using a computational color image analysis system (Leica Microscope DM2700M, Germany). Histological images were acquired from randomly selected fields, and the evaluation and quantitative analysis of histological changes were performed by investigators blinded to the experimental group allocation to minimize observer bias.

Evans Blue-TTC staining

After the mice were anesthetized, 0.5 % Evans Blue was injected via the external jugular vein. Once the body surface showed blue staining, 10% KCl was injected intravenously to arrest the heart in diastole. After perfusion, the heart was removed and rapidly frozen at -80 ˚C for 20 min. Using a blade, the heart was longitudinally cut into 4 slices (1 mm thick) from the apex to the base along the atrioventricular groove. The slices were incubated in 2% TTC solution at 37 ˚C in the dark, then fixed in 4% paraformaldehyde. Photographs were taken in anatomical order, and the proportions of the infarct area (INF, white area) and the area at risk (AAR, red area) were analyzed. The images were analyzed using ImageJ software by an investigator blinded to the experimental group allocation. The infarct size was calculated as the percentage of infarct area relative to the area at risk (INF/AAR×100 %).

Western blotting

The mouse apical tissue was homogenized in 0.5 ml of RIPA buffer (Biyuntian, Shanghai, China). It was shaken at 4 ˚C for 5 seconds, and this process was repeated 4 times. The dissolved protein was centrifuged at 13,500 rpm for 25 min, and the supernatant was collected. The protein concentration was quantified using a BCA protein assay kit (Biyuntian, Shanghai, China). The protein lysates from each group were separated by SDS-PAGE electrophoresis and transferred to PVDF membranes. The membranes were blocked with 5 % non-fat milk at room temperature for 2 hr, and then incubated with the following primary antibodies overnight at 4 ˚C (diluted at 1:500 or 1:1000): CD44 (Selleck, USA); Colα2 (III), PI3K, p-PI3K, VTN, Colα1 (III), α-SMA, AKT, p-AKT, FN1 (Sigma, USA); and GAPDH (Jingjie, Hangzhou, China). They were then incubated with anti-mouse IgG (Baisha, Beijing, China) or anti-rabbit IgG (Jingjie, Hangzhou, China) antibodies, diluted 1:10000, at room temperature for 1 hr. The specific complexes were detected using an enhanced chemiluminescence (ECL) kit (Baisha, Beijing, China) and a multi-fluorescence imaging system (Amersham Imager 600, GE, America). The gray values of the bands were quantified using ImageJ.

Bioinformatic analysis

Fold change of DEPs> 1.30 or<0.77 and *P*-value<0.05 were set as the significance thresholds. A volcano plot and hierarchical clustering analysis were carried out using Cluster 3.0 software. KEGG enrichment analysis and enrichment of Gene Ontology (GO) biological process, cellular component, and molecular function terms were performed using DAVID's Functional Annotation Chart tool (Version 6.8)(12, 13). DEPs were identified using predefined statistical criteria, and multiple testing was corrected with the Benjamini–Hochberg false discovery rate (FDR) method to control for false-positive findings. Fisher's exact test was used to analyze the association of categorical variables, with Benjamini–Hochberg correction applied where appropriate (FDR-adjusted $P<0.05$). Based on significantly enriched DEPs, heatmap visualization and hierarchical clustering analysis were performed using the heatmap.2 function in the "gplots" package of R software. Where applicable, effect estimates were reported together with 95% confidence intervals (95% CIs) in addition to *P*-values.

Statistical analysis

All experiments in this study were independently repeated at least 3 times, and the data are presented as mean ± standard deviation (SD). The normality of data distribution was assessed using the Shapiro–Wilk test. For comparisons between two groups, a two-tailed Student's t-test was applied for normally distributed data, whereas the Mann–Whitney U rank-sum test was used for non-normally distributed data. For comparisons among multiple groups, one-way ANOVA followed by Bonferroni's multiple comparison test was performed for normally distributed data, while the Kruskal–Wallis H test was used for non-normally distributed data. All statistical analyses were performed using GraphPad Prism 9.5 and SPSS 26.0 software. A two-tailed *P*-value <0.05 was considered statistically significant.

Results

IMP improves cardiac function in mice after MI

Electrocardiographic (ECG) findings demonstrated that approximately 5 min following isoproterenol (ISO) administration, mice in the ISO model group and all IMP treatment groups exhibited prominent T-wave inversion, a significant elevation in heart rate, and an absolute ST-segment deviation≥0.1 mV. Notably, IMP intervention mitigated the degree of T-wave inversion across all dosage groups. Furthermore, the absolute values of ST-segment deviation in the ISO+IMP 15 mg/kg and ISO+IMP 30 mg/kg groups decreased in a dose-dependent manner during the ischemic phase. Among these, the 30 mg/kg IMP dose exerted the most pronounced inhibitory effect on ST-segment deviation (Figure 1B-C). Echocardiography performed on days 1 and 7 after model establishment revealed that, compared with the Control group, mice in the ISO group exhibited a prolonged cardiac cycle (Figure 2A), markedly reduced left ventricular ejection fraction (LVEF) and fractional shortening (LVFS)(Figure 2B-C), increased left ventricular internal dimensions at diastole and systole (LVIDd and LVIDs)(Figure 2D-E), and decreased left ventricular anterior and posterior wall thickness during

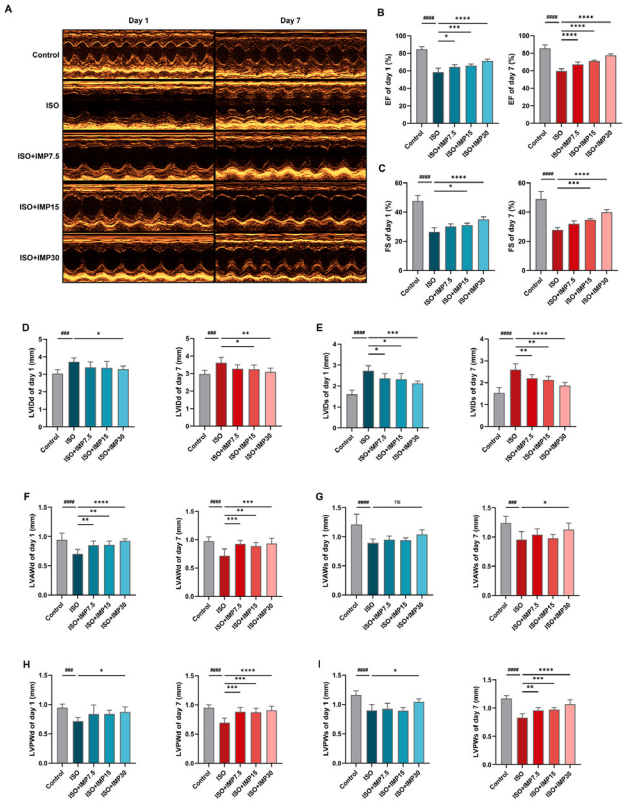

Figure 2. Effects of imperatorin (IMP) on echocardiographic findings and related indicators in mice after myocardial infarction (MI) on the 1st and 7th days

(A) Representative M-mode echocardiographic images of left ventricle on day 1 and day 7 in each group; (B) Left ventricular ejection fraction (EF); (C) Left ventricular fractional shortening (FS); (D) Left ventricular internal dimension end-diastole (LVIDd); (E) Left ventricular internal dimension end-systole (LVIDs); (F) Left ventricular anterior wall end-diastole (LVAWd); (G) Left ventricular anterior wall end-systole (LVAWs); (H) Left ventricular posterior wall end-diastole (LVPWd); (I) Left ventricular posterior wall end- systole (LVPWs) ($^{\#\#}P$<0.01, $^{\#\#\#\#}P$<0.0001 vs Control group, $^{*}P$<0.05,$^{**}P$<0.01,$^{***}P$<0.001,$^{****}P$<0.0001 vs ISO group, n=7)

diastole and systole (LVAWd, LVAWs, LVPWd, LVPWs) (Figures 2F-I). Notably, treatment with IMP at 30 mg/kg significantly reversed these structural and functional abnormalities, indicating a protective effect on cardiac remodeling following myocardial injury.

IMP alleviates myocardial injury and fibrosis in MI model mice

Serological tests indicated that at 24 hr after modeling (Figure 3A-B), LDH activity and cTn-I levels in the ISO group were significantly higher than in the Control group, whereas IMP treatment markedly reduced them in a dose-dependent manner. TTC staining results showed that compared with the Control group, the myocardial infarct size in the ISO group was significantly increased, and IMP intervention reduced the infarct size in a dose-dependent manner. Specifically, the 30 mg/kg IMP group (ISO+IMP30) showed a reduction of more than 50% in infarct size compared with the ISO group (Figure 3C-D). HE staining results revealed that in the Control group, the myocardial cell nuclei had a normal morphology and the myofibers were arranged tightly. In the ISO group, typical pathological changes were observed, including pyknosis/dissolution of myocardial cell nuclei, myofiber rupture and disorder, and interstitial inflammatory infiltration. In contrast, the ISO+IMP group significantly improved the structural damage and reduced inflammatory infiltration (Figure 3E). Masson trichrome staining confirmed that IMP significantly inhibited ISO-induced proliferation of myocardial interstitial collagen fibers, reduced the area of collagen deposition, and improved the extent of myocardial fibrosis after MI (Figure 3F). In conclusion, 30 mg/kg IMP exerts a cardioprotective effect on mice after MI through multiple pathways, whereby it significantly reduces the myocardial infarct size, alleviates myocardial injury, and inhibits the progression of myocardial fibrosis. Therefore, this dose was selected for subsequent mechanism-based studies.

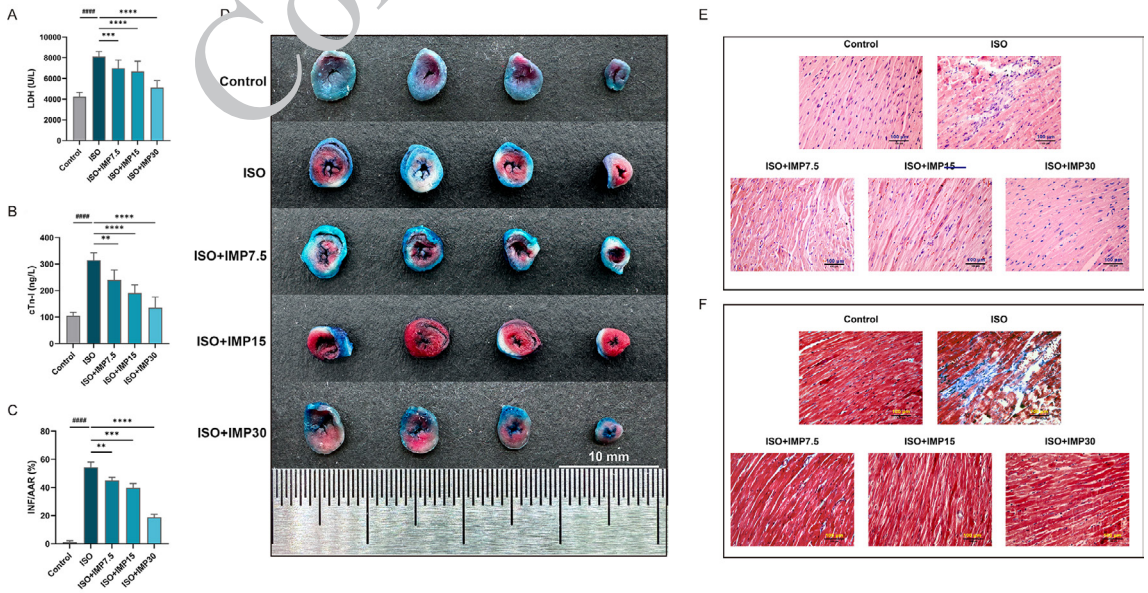

Figure 3. Imperatorin (IMP) attenuates myocardial injury and fibrosis in mice after myocardial infarction (MI)

(A) Effects of IMP on LDH activity in mouse serum on the first day after MI; (B) Effects of IMP on cTn-I content in mouse serum on the first day after MI; (C) Quantitative analysis of the proportions of infarcted area (INF) and area at risk (AAR) in heart sections; (D) Representative gross images of heart sections stained with Evans blue and triphenyltetrazolium chloride (TTC). The blue area indicates non-ischemic myocardium, the red area indicates ischemic but viable myocardium, and the pale white area indicates infarcted myocardium; (E) Representative hematoxylin-eosin (HE) staining images of myocardial tissues from each group; (F) Representative Masson's trichrome staining images of myocardial tissues from each group. Blue-stained areas indicate collagen deposition and fibrotic lesions ($^{####}P$<0.0001 vs Control group, $^{**}P$<0.01, $^{***}P$<0.001 and $^{****}P$<0.0001 vs ISO group)

Identification and cluster analysis of differentially expressed proteins (DEPs) in mouse heart tissues

Mass spectrometry analysis was performed on heart tissues from mice in the Control, ISO, and ISO+IMP (30 mg/kg) groups. A total of 28,171 peptides were identified, among which 27,730 were specific peptides. Additionally, 4,480 proteins were identified, with 4,466 proteins suitable for quantitative comparison (Figure 4B). Most peptides were 7-20 amino acids long, consistent with the general rules of enzyme digestion and mass spectrometry fragmentation. Furthermore, most proteins corresponded to more than two peptides, which improved the accuracy and reliability of the quantitative results (Figures 4C-D). A heat map was generated through cluster analysis to show the relative expression levels of DEPs in different samples. Compared with the Control group, the expression of a large number of proteins in heart tissues of the ISO group changed significantly (Figures 4A, F). A total of 98 DEPs were identified in the ISO/Control group, including 66 up-regulated and 32 down-regulated proteins. In the ISO+IMP/ISO group, 127 DEPs were identified, including 22 up-regulated and 105 down-regulated proteins (Figure 4E). Volcano plots were used to display the distribution of DEPs in the ISO/Control group and ISO+IMP/ISO group (Figures 4G-H), where red dots represent significantly up-regulated DEPs, blue dots represent significantly down-regulated DEPs, and gray dots represent proteins with no significant difference. These volcano plots suggest that the DEPs with significant differences may serve as potential biomarkers or therapeutic targets.

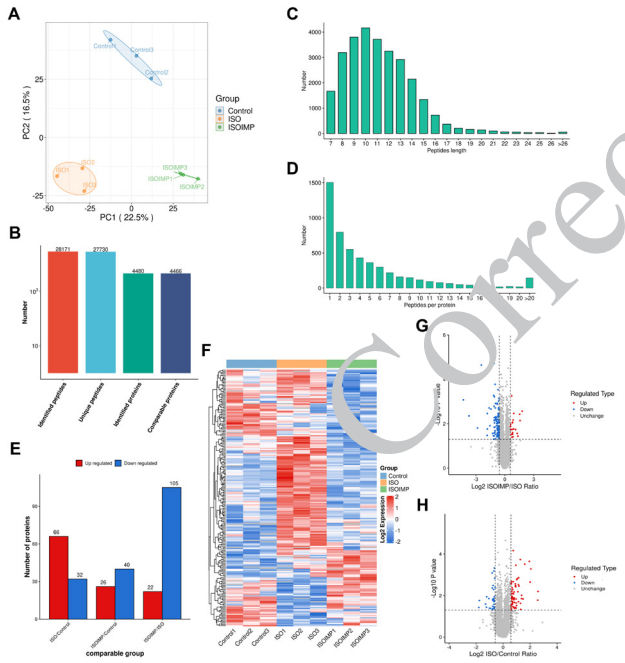

Figure 4. Identification of Differentially Expressed Proteins (DEPs) by mass spectrometry
(A) Principal component analysis (PCA) score plot showing the separation of protein expression profiles among control, ISO and ISO+IMP groups; (B) Statistical summary of identified peptides, unique peptides, identified proteins and comparable proteins from the proteomic dataset; (C) Length distribution of identified peptides; (D) Distribution of the number of peptides matched to each identified protein; (E) Number of up-regulated and down-regulated DEPs in three comparison pairs; (F) Hierarchical clustering heatmap of DEPs across all samples. Red indicates high expression and blue indicates low expression; (G) Volcano plot showing the expression of quantitative DEPs in heart tissues of mice from the ISO/Control group, with DEPs having a fold change > 1.5 marked by colors; (H) Volcano plot showing the expression of quantitative DEPs in heart tissues between the ISO+IMP/ISO group, with DEPs having a fold change >1.5 marked by colors
ISO: Isoproterenol; IMP: Imperatorin

Functional enrichment analysis of DEPs

Functional annotation and functional enrichment analyses of DEPs were performed using GO and KEGG. GO analysis showed that DEPs in the ISO/Control group and the ISO+IMP/ISO group were significantly enriched in the regulation of biological process, cellular component organization or biogenesis, response to chemical, extracellular region, and protein binding, etc. (Figure 5A-B). KEGG analysis revealed that DEPs in the ISO/Control group were enriched in multiple KEGG pathways, specifically in those related to organic systems and cellular processes. For instance, the up-regulated DEPs were enriched in pathways such as Complement and Coagulation Cascades, JAK-STAT Signaling Pathway, ECM-Receptor Interaction, and PI3K/AKT Signaling Pathway (Figure 5C); the down-regulated DEPs were enriched in Antigen Processing and Presentation (Figure 5E). In contrast, the up-regulated DEPs in the ISO+IMP/ISO group were enriched in pathways including Antigen Processing and Presentation (Figure 5D), while the down-regulated DEPs were enriched in pathways such as Complement and Coagulation Cascades and ECM-Receptor Interaction (Figure 5F). To further investigate the similarities and differences in the functions of DEPs among the three comparison groups, Gene Ontology (GO) and KEGG pathway clustering analyses were performed following functional classification and enrichment analysis of DEPs in these groups.

GO analysis revealed that DEPs in both the ISO/Control

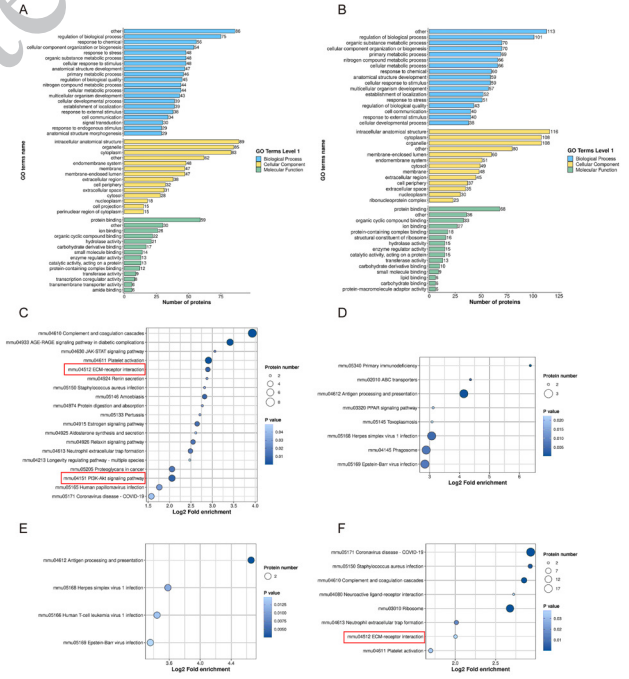

Figure 5. Functional enrichment analysis of DEPs in mice after myocardial infarction (MI)
(A) GO enrichment analysis of DEPs in the ISO vs Control group; (B) GO enrichment analysis of DEPs in the ISO+IMP vs ISO group. (C) KEGG pathway enrichment analysis of DEPs with up-regulated expression in the ISO/Control group; (D) KEGG pathway enrichment analysis of DEPs with up-regulated expression in the ISO+IMP/ISO group; (E) KEGG pathway enrichment analysis of DEPs with down-regulated expression in the ISO/Control group; (F) KEGG pathway enrichment analysis of DEPs with down-regulated expression in the ISO+IMP/ISO group
ISO: Isoproterenol; IMP: Imperatorin; GO: Gene ontology

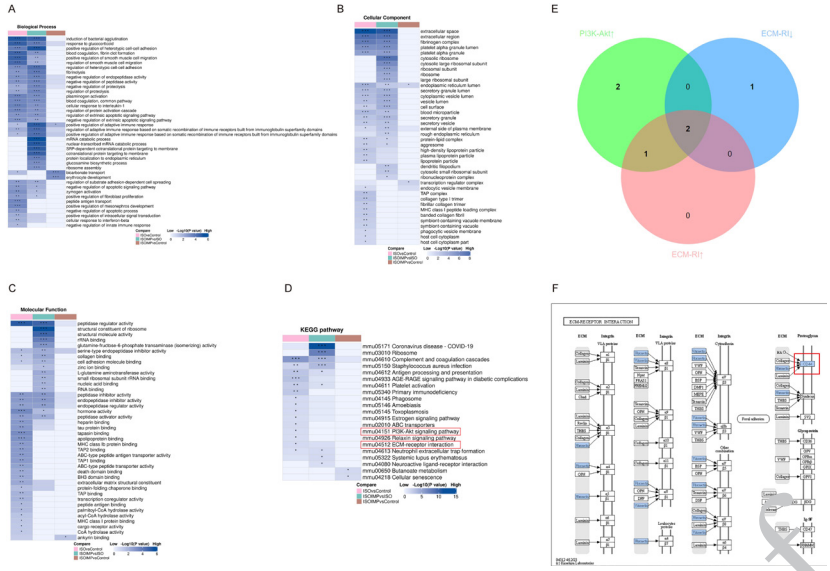

Figure 6. Functional enrichment clustering analysis of differentially expressed proteins (DEPs) among different mouse groups and analysis and visualization of DEPs enriched in relevant pathways

(A) Functional clustering analysis of DEPs in gene ontology (GO) biological process (BP); (B) Functional clustering analysis of DEPs in GO cellular component (CC); (C) Functional clustering analysis of DEPs in GO molecular function (MF); (D) Functional clustering analysis of DEPs in KEGG pathways; (E) Venn diagram of the union of DEPs enriched in the ECM-receptor interaction pathway and PI3K/AKT signaling pathway in the ISO/Control and ISO+IMP/ISO groups; (F) Down-regulation of CD44 protein in the ECM-receptor interaction pathway from the KEGG enrichment analysis in the ISO+IMP/ISO group, KEGG pathway (mmu04512) downloaded from the database (https://www.genome.jp/kegg/pathway.html)(*P<0.05, **P<0.01 and ***P<0.001)

ISO: Isoproterenol; IMP: Imperatorin; GO: Gene ontology

group and the ISO+IMP/ISO group were significantly enriched in terms including positive regulation of fibroblast proliferation, regulation of proteolysis, collagen binding, and ECM structural constituent, etc. (Figure 6A-C). KEGG clustering analysis indicated that DEPs in the ISO/Control group were significantly enriched in pathways including ECM-Receptor Interaction, PI3K/AKT Signaling Pathway, Complement and Coagulation Cascades, and Antigen Processing and Presentation (Figure 6D). Additionally, compared with mice in the ISO group, certain down-regulated DEPs in mice in the ISO+IMP group were also enriched in the process of positive regulation of fibroblast proliferation (Figure 6A).

A Venn diagram was constructed to illustrate the union of DEPs enriched in the ECM-receptor interaction and PI3K/AKT signaling pathways in the ISO/Control and ISO+IMP/ISO groups (Table 1, Figure 6E). It was revealed that there were 3 overlapping DEPs in these two pathways: (i) fibronectin 1 (FN1), (ii) vitronectin (VTN), and (iii) Colα2 (I), which not only serve as components of the ECM but are also enriched in the PI3K/AKT signaling pathway. Notably, the expression levels of these proteins were up-regulated in the ISO/Control group, whereas down-regulated in the ISO+IMP/ISO group. Additionally, in the ISO/Control group, the expression levels of the GTPase KRas (Kras) and Bcl2-related myeloid cell leukemia-1 (Mcl1), which are enriched in the PI3K/AKT signaling pathway, were up-regulated (Table 1). Moreover, CD44, a differential protein enriched in the ECM-receptor interaction pathway, was down-regulated in the ISO+IMP/ISO group CD44, was down-regulated (Figure 6F).

Protein-protein interaction (PPI) network analysis of differentially expressed proteins (DEPs) in mouse heart tissues

The top 50 proteins with the strongest interactions were screened from the ISO/Control group and the ISO+IMP/ISO group, respectively. Through PPI network analysis, several key hub proteins were identified, including FN1, VTN, CD44, Colα1 (III), and Colα2 (I). The results showed

Table 1. DEPs enriched in ECM-receptor interaction and PI3K/AKT signaling pathway in ISO/Control and ISO+IMP/ISO mouse groups

Protein ID	Gene Name	Fold Change (ISO/Control)/(ISO+IMP/ISO)	*P*_Value (ISO/Control)/(ISO+IMP/ISO)	Expression Levels (ISO/Control)/(ISO+IMP/ISO)
P11276	FN1	0.91355 / 0.98327	0.003339 / 0.0012174	Up / Down
P29788	VTN	2.00807 / 1.81469	0.0022538 / 0.003428	Up / Down
Q01149	Colα2 (I)	0.59678 / --	0.0296987 / --	Up / --
P15379	CD44	-- / 1.1095	-- / 0.0071161	-- / Down
P32883	KRas	0.76706 / --	0.0083675 / --	Up / --
P97287	Mcl1	0.72697 / --	0.007781 / --	Up / --

DEPs: Differentially expressed proteins; ISO: Isoproterenol; IMP: Imperatorin; ECM: Extracellular matrix

Table 2. Binding capacity of IMP to target protein CD44

Protein	PDBID	Ligand	Binding Affinity (kcal/mol)
CD44	4PZ3	IMP	-5.7

that the ECM component FN1 was significantly up-regulated in the ISO/Control group and located at the center of the interaction network, exhibiting close interactions with DEPs related to myocardial fibrosis such as VTN, Colα1 (III), and Colα2 (I)(Figure 7A). In the ISO+IMP/ISO group, FN1 was significantly down-regulated yet remained at the center of the interaction network, exhibiting close interactions with myocardial fibrosis-related DEPs (including VTN and Colα1 (III)) as well as CD44 (Figure 7B).

A Venn diagram was used to identify the intersection between the up-regulated DEPs in the ISO/Control group and the down-regulated DEPs in the ISO+IMP/ISO group; meanwhile, the intersection between the down-regulated DEPs in the ISO/Control group and the up-regulated DEPs in the ISO+IMP/ISO group was also determined. The results revealed a total of 48 DEPs that exhibited opposite expression trends between the ISO/Control group and the ISO+IMP/ISO group (Figures 7C-D). These 48 overlapping genes were imported into the STRING database for PPI network analysis, and the PPI network was visualized using Cytoscape 3.9.1 software. The results indicated that among these DEPs with opposite expression trends, FN1 was located at the center of the interaction network and had close interactions with myocardial fibrosis-related DEPs such as VTN and Colα1 (III)(Figures 7E-F).

Results of molecular docking and expression levels of fibrosis-related DEPs

To determine whether CD44 is a potential molecular target of IMP, molecular docking analysis was performed. The results showed a binding energy of -5.7 kcal/mol between CD44 and IMP (Table 2), indicating strong binding affinity. The predicted binding conformation of IMP within the CD44 protein was further visualized and optimized using PyMOL (Figure 8A), supporting the likelihood that

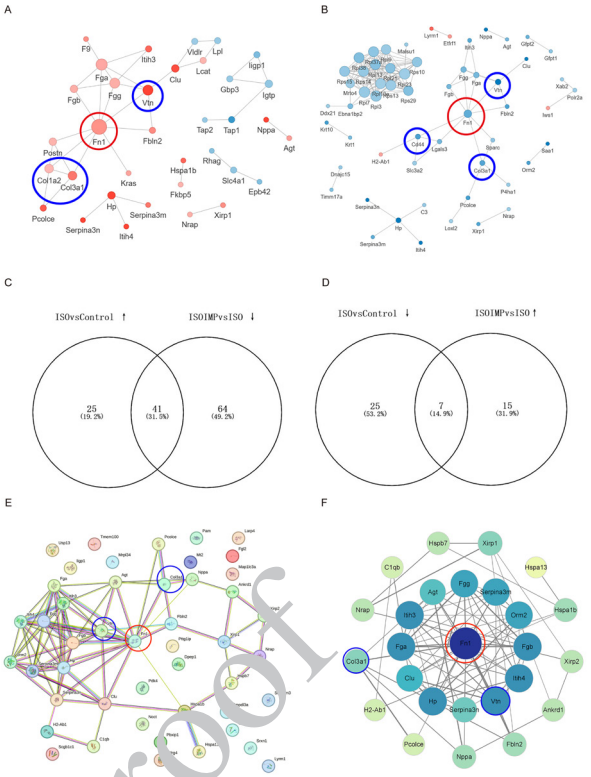

Figure 7. Protein-protein interaction (PPI) network analysis of differentially expressed proteins (DEPs) in mouse heart tissues
(A-B) PPI network of DEPs in the ISO vs Control comparison; PPI network of DEPs in the ISO+IMP/ISO group (fold change >1.5, confidence >0.7, blue and red represent down-regulated and up-regulated proteins, respectively, with darker colors indicating larger fold changes; the size of the circles represents the number of interacting proteins ; (C) Venn diagram showing the intersection of up-regulated proteins in ISO vs Control and down-regulated proteins in ISO+IMP vs ISO; (D) Venn diagram showing the intersection of down-regulated proteins in ISO vs Control and up-regulated proteins in ISO+IMP vs ISO; (E) PPI network analyzed by the STRING database; (F) PPI network further visualized using Cytoscape
ISO: Isoproterenol; IMP: Imperatorin

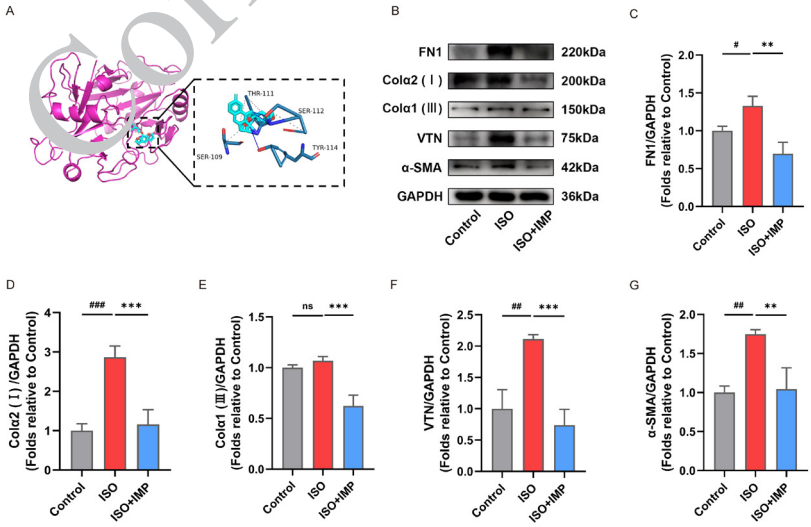

Figure 8. Molecular docking and effects of IMP on the expression levels of fibrosis-related proteins FN1, VTN, Colα1 (III), Colα2 (I), and α-SMA in myocardial tissues of each mouse group
(A) Molecular docking result showing the binding mode of Imperatorin with the protein CD44. The magnified view displays the detailed interaction between Imperatorin (cyan) and key amino acid residues (blue) in the protein binding pocket. (B) Representative Western blot bands of fibrosis-related proteins; (C-G) Quantitative analysis of relative protein expression levels of FN1, Colα2 (I), Colα1 (III), VTN and α-SMA, normalized to GAPDH in myocardial tissues of each group ($^{\#}P<0.05$, $^{\#\#}P<0.01$, $^{\#\#\#\#}P<0.0001$ vs Control; $^{**}P<0.01$ and $^{***}P<0.001$ vs ISO; n=3)

CD44 is a direct target of IMP. To validate the effects of IMP on myocardial fibrosis in mice post-MI and to ensure the reliability of the proteomic findings, Western blot analysis was performed to assess key DEPs (Figure 8B). The results demonstrated that, in comparison with the Control group, the expression levels of FN1, VTN, Colα2 (I), and α-SMA proteins in the myocardial tissue of mice in the ISO group were significantly elevated, while the expression levels of Colα1 (III) protein exhibited an upward trend (P>0.05). In contrast to the ISO group, the protein levels of FN1, VTN, Colα1 (III), Colα2 (I), and the fibroblast marker α-SMA were significantly reduced in the myocardial tissue of mice in the ISO+IMP group (Figure 8C-G).

Expression levels of CD44 and PI3K/AKT pathway-related proteins

To investigate the effect of IMP on CD44 and the proteins associated with the enriched pathway, additional Western blot analyses were performed (Figure 9A). The results indicated that, relative to the Control group, the expression level of the phosphorylated PI3K (p-PI3K) protein was significantly increased in the myocardial tissue of mice in the ISO group, while CD44 and phosphorylated AKT (p-AKT) proteins showed an upward trend, consistent with the proteomic results. Compared with the ISO group, the expression levels of CD44, p-PI3K, and p-AKT proteins in the myocardial tissue of mice in the ISO + IMP group were significantly decreased. These results further validated the down-regulation of CD44 observed in the proteomics analysis and revealed that IMP treatment was accompanied by reduced phosphorylation of PI3K/AKT pathway-related proteins (Figure 9B-D).

Discussion

The present study demonstrates that IMP exerts a cardioprotective effect against isoprenaline (ISO)-induced MI injury in mice. Administration of IMP significantly improved cardiac function, reduced myocardial infarct size, preserved myocardial histological architecture, alleviated myocardial fibrosis, and decreased serum levels of myocardial marker enzymes in mice with ISO-induced myocardial injury. ISO is a non-selective β-adrenergic receptor agonist that induces oxidative stress, inflammatory responses, and perturbations in calcium ion homeostasis via excessive receptor activation, thereby leading to myocardial cell damage and fibrosis (14). These processes are primarily characterized by the excessive deposition of type I and type III collagen (Col I and Col III) and activation of cardiac fibroblasts(15). Contextually, ISO-induced myocardial injury has been widely used to investigate the effect of drugs on MI. In the present study, we systematically explored the cardioprotective mechanism of IMP using an ISO-induced mouse model of MI, in conjunction with proteomic analysis and experimental validation.

Challa *et al.* demonstrated that two consecutive injections of ISO at a dose of 50 mg/kg/day can induce both MI and myocardial fibrosis in mice (16). Accordingly, in our study, we administered two consecutive injections of ISO at 50 mg/kg/day to establish the mouse MI model. The results of this study demonstrated that following ISO injection, mice displayed ECG alterations characterized by T-wave inversion and ST-segment deviation with an absolute value ≥0.1 mV. Meanwhile, serum cTn-I levels and LDH activity were significantly elevated. Cardiac function indices, including LVAW, LVPW, LVEF, and LVFS, were all decreased, whereas the LVID was increased. Evans Blue-TTC double staining revealed a marked enlargement of the myocardial infarct size. H&E staining revealed that, following MI induction, some myocardial nuclei exhibited pyknosis, karyorrhexis, and karyolysis; myocardial cells and muscle fibers were disorganized, with evident fiber distortion and rupture, accompanied by interstitial inflammatory cell infiltration, confirming the successful establishment of the MI model. Furthermore, treatment with IMP

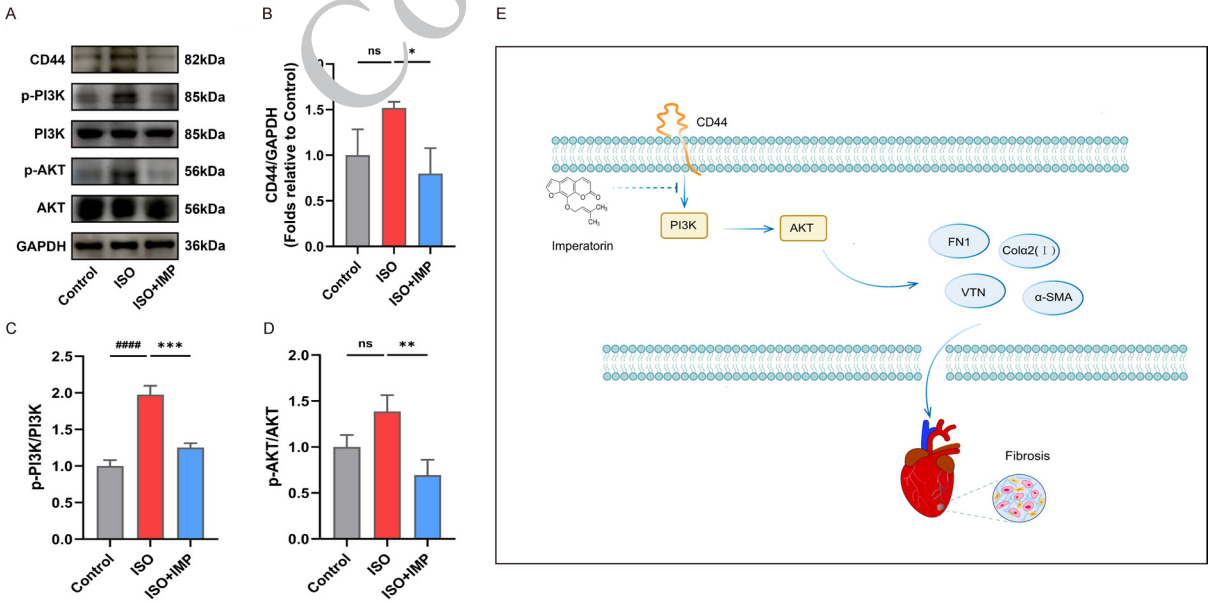

Figure 9. Effects of imperatorin (IMP) on the expression levels of t PI3K/AKT pathway-related proteins
(A) Representative Western blot bands of CD44, p-PI3K, PI3K, p-AKT and AKT; (B-D) Quantitative analysis of relative protein expression levels of CD44, p-PI3K, p-AKT, normalized to GAPDH or PI3K, AKT in myocardial tissues of each group; (E) Schematic diagram showing the mechanism of IMP alleviating Post-Infarction Cardiac Fibrosis (####P<0.0001 vs Control; *P<0.05, **P<0.01 and ***P<0.001 vs ISO; n=3)

significantly ameliorated these histopathological changes in a dose-dependent manner, improved cardiac function, and mitigated myocardial tissue damage. Further histological analyses demonstrated that IMP reduced infarct size and suppressed inflammatory infiltration. These effects align with previously reported anti-inflammatory actions of IMP in pulmonary fibrosis via the NF-κB/JAK–STAT signaling pathway (17). Collectively, these multi-targeted protective effects provide strong experimental evidence supporting the therapeutic potential of IMP in ameliorating MI.

The heart is composed of a variety of cell types, including cardiomyocytes, cardiac fibroblasts (CFs), endothelial cells (ECs), pericytes, and immune cells. Myocardial fibrosis occurring after MI induces adverse ventricular remodeling and heart failure, in which CFs play a central role(18). Following myocardial ischemia and hypoxia, a large number of CFs are recruited and activated, and then differentiate into α-SMA-expressing myofibroblasts. These myofibroblasts synthesize excessive amounts of type I and type III collagen, resulting in scar tissue formation and ECM accumulation. The newly formed scar tissue replaces the infarcted myocardium, thereby progressively exacerbating myocardial fibrosis. A study by Matsuda *et al.* demonstrated that IMP attenuates hypertension-induced cardiac fibrosis by reducing collagen accumulation and oxidative stress by inhibiting fibrosis-related signaling pathways such as TGF-β_1 and MMP-2 in myocardial tissue and the surrounding microvasculature (19). Other studies have indicated that IMP reduced myocardial hypertrophy and fibrosis by up-regulating eNOS signaling, thereby inhibiting myocardial remodeling (20). Our results demonstrated an increased deposition of blue-stained collagen fibers in the myocardial tissue of mice following ISO injection, indicating that MI promotes ECM accumulation and consequent myocardial fibrosis. However, IMP treatment significantly inhibited collagen fiber deposition in the myocardial injury site, suggesting that IMP improves post-MI myocardial fibrosis through its anti-fibrotic effects, potentially by suppressing myofibroblast activation and ECM deposition. These findings are consistent with the proteomic analysis, which revealed significant changes in the expression levels of fibrosis-related DEPs following IMP intervention. Notably, these DEPs are involved in ECM organization and collagen synthesis, further supporting IMP's inhibitory role in myocardial fibrotic remodeling.

To elucidate the therapeutic mechanism of IMP in MI, we employed 4D label-free quantitative proteomics to identify key ECM molecules associated with fibrosis. PPI network analysis revealed FN1 as a hub protein that was significantly up-regulated in the ISO-treated group and formed a closely interacting cluster with VTN, Colα1(III), and Colα2(I). FN1 is known to promote collagen assembly through integrin-mediated interactions (21), and its overexpression has been directly linked to ischemic myocardial fibrosis. Notably, IMP treatment significantly down-regulated FN1 expression. VTN, primarily secreted by activated macrophages and implicated in fibroblast activation (22), was also significantly up-regulated in the ISO group, while IMP intervention effectively reversed this increase. Consistent with these findings, the deposition of Colα1(III) and Colα2(I) was markedly increased in the ISO group; however, it was significantly attenuated by IMP treatment. Additionally, proteomic analysis identified CD44 as a key ECM receptor that was up-regulated in the ISO group and reduced following IMP administration. Western blot validation further confirmed that IMP simultaneously inhibited α-SMA and the aforementioned ECM molecules. Collectively, these results indicate that IMP inhibits cardiac fibroblast activation and collagen deposition by modulating the core ECM molecular network comprising FN1, VTN, Collagens, and CD44, thereby ameliorating myocardial fibrosis.

CD44 is a transmembrane receptor glycoprotein widely expressed in diverse cell types, including leukocytes and fibroblasts. It can bind to a range of ECM proteins, including hyaluronic acid (HA)(23). Studies have demonstrated that CD44, through its interaction with HA, plays a key role in ECM remodeling, tissue fibrosis, myofibroblast proliferation, and the progression of heart failure (24). Additionally, Tong W *et al.* (25) reported that the CD44 receptor on hepatic stellate cells interacts with SPP1 derived from hepatocellular carcinoma (HCC) cells, thereby activating the PI3K/AKT signaling pathway and promoting the differentiation of hepatic stellate cells (HSCs) into cancer-associated fibroblasts (CAFs). This finding suggests that inhibiting the PI3K/AKT pathway in fibroblasts can effectively hinder their activation and transformation. Collectively, these findings suggest that interactions between CD44 and its ligands can activate fibroblasts and drive their transformation via the PI3K/AKT signaling pathway. However, it remains unclear whether CD44 facilitates the migration of CFs after MI and their subsequent excessive transformation into myofibroblasts by activating the PI3K/AKT signaling pathway. Therefore, we conducted further experiments to verify this hypothesis.

KEGG enrichment analysis revealed significant enrichment of the PI3K/AKT signaling pathway in the ISO group, while IMP treatment attenuated this enrichment. Although transient activation of the PI3K/AKT pathway exerts a cardioprotective effect during the early stages of myocardial injury (26), sustained activation has been shown to exacerbate CFs proliferation and fibrosis (26). Consistent with these observations, the present study confirmed that ISO administration significantly increased the phosphorylation levels of PI3K and AKT, while IMP treatment effectively suppressed their phosphorylation. Notably, FN1, VTN, and Colα2(I) are shared molecular components of both the PI3K/AKT and ECM-receptor pathways, suggesting that these signaling pathways may synergistically promote fibrosis by regulating overlapping targets. CD44, a key molecule in the ECM-receptor interaction pathway, showed expression changes that closely correlated with alterations in PI3K/AKT activity. Similarly, a study by Chi *et al.* (27) demonstrated that pentraxin 3 (PTX3) activates signaling pathways such as PI3K/AKT1 through the CD44 axis, thereby promoting myofibroblast transactivation and collagen accumulation, and exacerbating pulmonary fibrosis. In the current study, proteomic analysis identified CD44 as a core DEP that was significantly up-regulated in the MI model and exhibited close interactions with ECM components, including FN1 and collagens. Molecular docking results further confirmed a strong binding affinity between CD44 and IMP, and IMP treatment effectively reversed the MI-induced CD44 up-regulation, suggesting that CD44 may serve as a direct molecular target of IMP. Based on the integrated analysis of the biological processes, core targets, and core pathways

underlying the anti-myocardial fibrosis effect of IMP, we propose that IMP attenuates post-MI myocardial fibrosis by down-regulating the CD44/PI3K/AKT signaling pathway and inhibiting the proliferation, activation, and migration of CFs. These findings highlight the importance of the CD44/PI3K/AKT pathway as a potential therapeutic target for fibrotic diseases (Figure 9E).

Although IMP exhibited promising cardioprotective effects in our mouse model, there are still some limitations. First, this study was based on a single animal model, and further validation in other models is required. In addition, the clinical translation of IMP doses remains uncertain due to interspecies differences. Further pharmacokinetic studies are needed to evaluate its bioavailability and therapeutic feasibility. Second, systematic evaluation of acute and chronic toxicity, safety margins, and optimized delivery strategies will be essential. Therefore, while IMP represents a promising candidate for preventing cardiac fibrosis, additional preclinical studies and clinical investigations are required to validate its safety, efficacy, and translational potential. Third, although our results suggest that the CD44/PI3K/AKT pathway may mediate the anti-fibrotic effects of IMP, further *in vitro* studies using CD44 gene knockout and PI3K/AKT pathway inhibitors are required to confirm causality and elucidate the underlying molecular mechanisms. Moreover, the relatively short observation period limits the assessment of long-term cardiac remodeling.

Conclusion

Imperatorin attenuates post-infarction cardiac fibrosis in mice. Its protective effects may involve CD44/PI3K/AKT signaling and other pathways identified through proteomic analysis, which require further validation.

Acknowledgment

This work was supported by the Heilongjiang Natural Science Foundation project (No. SS2023H003); Heilongjiang Province Traditional Chinese Medicine Research Project (No. ZHY2024-212); Basic Scientific Research Business Research Project of Heilongjiang (No. 2024-KYYWF-0502); Program for Young Talents of Basic Research in Universities of Heilongjiang Province (No. YQJH2025260).

Data Availability Statement

The data supporting the findings of this study are available from the corresponding author upon reasonable request. The proteomics data presented in this study were provided by Jingjie Biotechnology Co., Ltd. The relevant repository and accession number are as follows: Proteomics Identifications Database (PRIDE Database) with accession PXD069342.

Authors' Contributions

J S and H Y conceived and designed the study, collected and analyzed data, and drafted the initial manuscript. MA A, YY Y, X L, J Q, MY W, YY Z, and TT L carried out the experiments. YK H carried out the data analysis. All authors approved the submission of this manuscript and agree to take responsibility for all aspects of the study.

Conflicts of Interest

The authors declare no competing interests.

Declaration

We have not used any AI tools or technologies to prepare this manuscript

References

1. Jimenez SA, Mendoza FA, Piera-Velazquez S. A review of recent studies on the pathogenesis of Systemic Sclerosis: Focus on fibrosis pathways. Front Immunol 2025; 16: 1551911.
2. Weng L, Ye J, Yang F, Jia S, Leng M, Jia B, *et al.* TGF-β1/SMAD3 regulates programmed cell death 5 that suppresses cardiac fibrosis post-myocardial infarction by inhibiting HDAC3. Circ Res 2023; 133: 237-251.
3. Tani H, Sadahiro T, Yamada Y, Isomi M, Yamakawa H, Fujita R, *et al.* Direct reprogramming improves cardiac function and reverses fibrosis in chronic myocardial infarction. Circulation 2023; 147: 223-238.
4. Yang JD, Lin SC, Kuo HL, Chen YS, Weng PY, Chen CM, *et al.* Imperatorin ameliorates ferroptotic cell death, inflammation, and renal fibrosis in a unilateral ureteral obstruction mouse model. Phytomedicine 2024; 135: 156066.
5. Ge JW, Deng SJ, Xue ZW, Liu PY, Yu LJ, Li JN, *et al.* Imperatorin inhibits mitogen-activated protein kinase and nuclear factor kappa-B signaling pathways and alleviates neuroinflammation in ischemic stroke. CNS Neurosci Ther 2022; 28: 116-125.
6. Zhang Y, Cao Y, Duan H, Wang H, He L. Imperatorin prevents cardiac hypertrophy and the transition to heart failure via NO-dependent mechanisms in mice. Fitoterapia 2012; 83: 60-66.
7. Zhang R, Wang F, Jin Y, Xie Q, Xiao P. Imperatorin's effect on myocardial infarction based on network pharmacology and molecular docking. Cardiovasc Ther 2025; 2025: 7551459.
8. Sun GZ, Meng FJ, Cai HQ, Diao XB, Zhang B, Bai XP. Ginsenoside Rg3 protects heart against isoproterenol-induced myocardial infarction by activating AMPK mediated autophagy. Cardiovasc Diagn Ther 2020; 10: 153-160.
9. Cabello JB, Burls A, Emparanza JI, Bayliss S, Quinn T. Oxygen therapy for acute myocardial infarction. Cochrane Database Syst Rev 2016; 12: Cd007160.
10. Liao XY, Liu P, Luo TF, Li Y, Gao Y, Pan FY, *et al.* Punicalagin attenuates isoproterenol-induced myocardial infarction through nuclear factor erythroid 2-related factor 2/silent information regulator transcript-1-mediated inhibition of inflammation and cardiac stress markers in experimental animal models. J Physiol Pharmacol 2024; 75: 123-136.
11. Elseweidy MM, Ali SI, Shaheen MA, Abdelghafour AM, Hammad SK. Vanillin and pentoxifylline ameliorate isoproterenol-induced myocardial injury in rats via the Akt/HIF-1α/VEGF signaling pathway. Food Funct 2023; 14: 3067-3082.
12. Sun Y, Zhang L, Lu B, Wen J, Wang M, Zhang S, *et al.* Hydrogen sulphide reduced the accumulation of lipid droplets in cardiac tissues of db/db mice via Hrd1 S-sulfhydration. J Cell Mol Med 2021; 25: 9154-9167.
13. Zhang Y, Zhang S, Li B, Luo Y, Gong Y, Jin X, *et al.* Gut microbiota dysbiosis promotes age-related atrial fibrillation by lipopolysaccharide and glucose-induced activation of NLRP3-inflammasome. Cardiovasc Res 2022; 118: 785-797.
14. Gruber R, Leimer M, Fischer MB, Agis H. Beta2-adrenergic receptor agonists reduce proliferation but not protein synthesis of periodontal fibroblasts stimulated with platelet-derived growth factor-BB. Arch Oral Biol 2013; 58: 1812-1817.
15. Bader Eddin L, Nagoor Meeran MF, Kumar Jha N, Goyal SN, Ojha S. Isoproterenol mechanisms in inducing myocardial fibrosis and its application as an experimental model for the evaluation of therapeutic potential of phytochemicals and pharmaceuticals. Animal Model Exp Med 2025; 8: 67-91.
16. Challa AA, Vukmirovic M, Blackmon J, Stefanovic B. Withaferin-A reduces type I collagen expression in vitro and inhibits development of myocardial fibrosis *in vivo*. PLoS One 2012; 7: e42989.
17. Li YZ, Chen JH, Tsai CF, Yeh WL. Anti-inflammatory property of imperatorin on alveolar macrophages and inflammatory lung

injury. J Nat Prod 2019; 82: 1002-1008.
18. Chen KJ, Zhang Y, Zhu XY, Yu S, Xie Y, Jin CJ, *et al.* GSTM1 suppresses cardiac fibrosis post-myocardial infarction through inhibiting lipid peroxidation and ferroptosis. Mil Med Res 2025; 12: 26.
19. Matsuda H, Morikawa T, Ohgushi T, Ishiwada T, Nishida N, Yoshikawa M. Inhibitors of nitric oxide production from the flowers of *Angelica furcijuga*: Structures of hyuganosides IV and V. Chem Pharm Bull (Tokyo) 2005; 53: 387-392.
20. Nasser MI, Zhu S, Hu H, Huang H, Guo M, Zhu P. Effects of imperatorin in the cardiovascular system and cancer. Biomed Pharmacother 2019; 120: 109401.
21. Stachowicz A, Sadiq A, Walker B, Sundararaman N, Fert-Bober J. Treatment of human cardiac fibroblasts with the protein arginine deiminase inhibitor BB-Cl-amidine activates the Nrf2/HO-1 signaling pathway. Biomed Pharmacother 2023; 167: 115443.
22. Peng Y, Li L, Shang J, Zhu H, Liao J, Hong X, *et al.* Macrophage promotes fibroblast activation and kidney fibrosis by assembling a vitronectin-enriched microenvironment. Theranostics 2023; 13: 3897-3913.
23. Perschl A, Lesley J, English N, Hyman R, Trowbridge IS. Transmembrane domain of CD44 is required for its detergent insolubility in fibroblasts. J Cell Sci 1995; 108: 1033-1041.
24. Suleiman M, Abdulrahman N, Yalcin H, Mraiche F. The role of CD44, hyaluronan and NHE1 in cardiac remodeling. Life Sci 2018; 209: 197-201.
25. Tong W, Wang T, Bai Y, Yang X, Han P, Zhu L, *et al.* Spatial transcriptomics reveals tumor-derived SPP1 induces fibroblast chemotaxis and activation in the hepatocellular carcinoma microenvironment. J Transl Med 2024; 22: 840.
26. Zhong S, Guo H, Wang H, Xing D, Lu T, Yang J, *et al.* Apelin-13 alleviated cardiac fibrosis via inhibiting the PI3K/Akt pathway to attenuate oxidative stress in rats with myocardial infarction-induced heart failure. Biosci Rep 2020; 40: BSR20200040.
27. Chi JY, Hsiao YW, Liang HY, Huang TH, Chen FW, Chen CY, *et al.* Blockade of the pentraxin 3/CD44 interaction attenuates lung injury-induced fibrosis. Clin Transl Med 2022; 12: e1099.